Analysis of the ac Free Electron Laser

TAE HUN CHUNG AND JIN HYUN LEE

***Abstract*—A free-electron laser with an ac electric wiggler is analyzed using linear fluid theory. The dispersion relation, the growth rate of the instability, and the efficiency of the laser are formulated, and the operating regimes are then investigated by a study of the parameters. Gain calculation according to the Madey theorem is also performed.**

I. Introduction

Stimulated emission of backscattered radiation from intense relativistic electron beams has been the subject of considerable interest in the past few years [1]–[8]. The free electron laser (FEL) is a device which operates via the stimulated backscattering of a low-frequency wave from the "free" particles of a relativistic electron beam. The primary reason for interest in the FEL is that the backscattered radiation from a relativistic electron beam can undergo a dramatic upshift of the order of γ_0^2, and is readily tunable over a wide frequency range [9].

The two principal types of scattering processes which occur in FEL experiments are wave–particle (Compton) scattering and wave–wave (Raman) scattering. If in laboratory frame a relativistic electron beam has a drifting Maxwellian distribution in its momentum space with a half-width ΔP, then the scattering parameter $k\lambda_D$, is written as [10]

$$k\lambda_D = 2\sqrt{\gamma_0} k_0 \Delta P / m_0 \omega_{pe}.$$

If $k\lambda_D > 1$, the system is in the stimulated Compton regime and fluid theory is not valid.

For valid application of the fluid theory, the condition $k\lambda_D < 1$ should be satisfied, that is, the system should be in the stimulated Raman scattering regime. This condition requires a cold beam (small ΔP), an intense electron beam ($I > 1$ kA), and relatively low electron energy ($\gamma_0 < 10$) [11].

In this paper, the relativistic factor, γ_0, of the electron beam generally ranges from 9 to 50. For linear fluid theory to be applied, the densities of the electron beam have to be kept higher than 10^{16} cm^{-3}.

The FEL, which is composed of a completely nonneutralized relativistic electron beam propagating along the z axis of a static helical wiggler magnetic field, has long been the subject of study [7]–[9]. In order to increase beam currents, an axial homogeneous magnetic field much stronger than the self-field of the electron beam is applied [10]–[14]. Unfortunately, there is a limitation in the FEL action. The high magnetic field strengths needed for such wigglers are not attainable with present technology for conventional static wigglers with wavelengths less than 1 cm. Operation at wavelengths shorter than this, therefore, would require a large increase in the number of wiggler periods. But in this case the extraction efficiency is low, and a very small electron beam energy spread and emittance are required.

In order to supply much shorter wavelengths in the FEL configuration, purely electric wigglers, which are of two types, are introduced [15], [16]. One, called the ac FEL, uses superconductor cavities which can supply ac fields of frequency $f_0 > 10$ GHz with amplitude $E_{\max} > 20$ MV/m. This is equivalent to a wiggler magnetic field of 700 G in the conventional FEL and may form the basis of a new class of submillimeter- or even visible-regime devices [15]. The other uses a plasma medium which can supply a relativistic plasma density wave. The plasma wiggler consists of a purely electric field oscillating with a frequency ω_p; the field is perpendicular to the electron beam propagation but has no spatial dependence since $\boldsymbol{k}$ of the radiation is transverse to $\boldsymbol{k}_p$. The geometry of the plasma wiggler is illustrated in Fig. 1. The effective wiggler wavelength becomes short (about order 100 μm), and the effective wiggler strength can be extremely large, namely 1 MG, with wiggler fields at 100-μm wavelength. Therefore, the FEL action ranges from the visible to the UV regime [16].

In Section II, the dispersion relation is derived from linear fluid theory in the stimulated Raman regime. Then the growth rate of the electromagnetic instability and the efficiency of the laser are calculated. In Section III, we perform a gain calculation according to the Madey theorem. In Section IV, operating regimes of several parameters in this FEL are investigated. Finally, conclusions are listed and discussed in Section V.

II. Theory and Analysis

In this system, consider a transversely homogeneous, nonneutralized relativistic electron beam with the velocity in the z direction, v_{0z}, moving through a spatially uniform, transversely oscillating electric field

$$\boldsymbol{E} = E_p \sin(\omega_p t)\boldsymbol{a}_x \tag{1}$$

where E_p is the amplitude of the electric wiggler field. This electric field may be an ac field in the superconductor

Manuscript received September 7, 1989; revised February 22, 1990. This work was supported by the Korea Science and Engineering Foundation.

The authors are with the Department of Physics, Dong-A University, Hadandong, Saha-Gu, 604-714, Pusan, Korea.

IEEE Log Number 9035710.

0093-3813/90/0600-0651$01.00 © 1990 IEEE

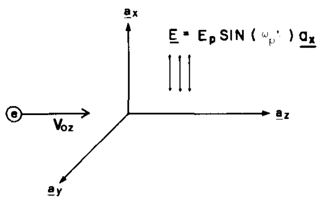

Fig. 1. Geometry of the electric wiggler FEL.

cavity or a relativistic plasma density wave excited in the plasma medium. In the electron frame, the electric field looks like an intense electromagnetic pump wave, and under proper circumstances, parametric instability can take place.

Choosing the Coulomb gauge, $\nabla \cdot \boldsymbol{A} = 0$, Ampere's law for the transverse component yields the wave equation

$$\left(\frac{\partial^2}{\partial z^2} - \frac{1}{c^2}\frac{\partial^2}{\partial t^2}\right)\boldsymbol{A}_\perp = -\frac{4\pi}{c}\boldsymbol{j}_\perp \tag{2}$$

which relates the transverse component of the vector potential to the transverse component of the current density.

We adopt a linearization of the form $\boldsymbol{A}_\perp = \boldsymbol{A}_{0\perp} + \boldsymbol{A}'_\perp$, $\boldsymbol{j}_\perp = \boldsymbol{j}_{0\perp} + \boldsymbol{j}'_\perp$, where $\boldsymbol{A}_{0\perp}$ and $\boldsymbol{A}'_\perp$ are the zeroth-order and the first-order vector potential, respectively, and $\boldsymbol{j}_{0\perp}$ and $\boldsymbol{j}'_\perp$ are the zeroth-order and the first-order current density, respectively.

The motion of the electron beam in the electromagnetic field and the oscillating electric field is governed by the equation

$$\frac{d\boldsymbol{P}}{dt} = -e\left[\boldsymbol{E} + \frac{\boldsymbol{v} \times \boldsymbol{B}}{c}\right] - \frac{1}{n_0}\nabla \cdot \mathsf{P} \tag{3}$$

where $\boldsymbol{B}$ is the total magnetic field, P is the stress tensor, and n_0 is the zeroth-order electron density. In the following, it is assumed that the beam is sufficiently tenuous, so that the beam self-fields may be neglected in the analysis; however, the perturbed fields resulting from longitudinal particle bunching will be retained. Because the electron beam is assumed to be drifting Maxwellian, we have retained only the longitudinal component of the stress tensor in the equation of motion to provide the approximate thermal contribution.

Since the system is assumed to be uniform in the transverse directions, it follows that the transverse canonical momentum of a particle is a constant of the motion, i.e.,

$$\boldsymbol{P}'_\perp = \frac{e}{c}\boldsymbol{A}'_\perp \tag{4}$$

where $\boldsymbol{P}'_\perp$ is the first-order perturbation of the transverse kinetic momentum. The perturbered current density is also given by

$$\boldsymbol{j}'_\perp = -e(n_0\boldsymbol{v}'_\perp + n'\boldsymbol{v}_{0\perp}) \tag{5}$$

where n_0 and n' are the zeroth-order and first-order electron densities.

From (3) the zeroth-order response of an electron through the electric field is simply

$$\boldsymbol{v} = v_{0z}\boldsymbol{a}_z + \frac{eE_p}{m_0\gamma_0\omega_p}\cos(\omega_p t)\boldsymbol{a}_x \tag{6}$$

where γ_0 is the relativistic factor.

Substituting (4) and (5) into the linearized form of (2),

$$\left(\frac{\partial^2}{\partial z^2} - \frac{1}{c^2}\frac{\partial^2}{\partial t^2}\right)\boldsymbol{A}'_\perp = -\frac{4\pi}{c}\boldsymbol{j}'_\perp \tag{7}$$

yields

$$\left(\frac{\partial^2}{\partial z^2} - \frac{1}{c^2}\frac{\partial^2}{\partial t^2} - \frac{\omega_{pe}^2}{\gamma_0 c^2}\right)\boldsymbol{A}'_\perp = \frac{4\pi e n'}{c}\boldsymbol{v}_{0\perp} \tag{8}$$

where ω_{pe} is the plasma frequency of the electron beam.

Assume all the perturbed quantities have the form:

$$\xi = \sum_k \xi_k \exp\left[i(kz - \omega t)\right] \tag{9}$$

where $\xi = n', v'_\perp, A'_\perp, j'_\perp, E'_x$, and E'_z.

From (8) and (9), we obtain the equation

$$A'_{x,k} = -\frac{2\pi c e^2 E_p}{m_0\gamma_0\omega_p\omega^2\epsilon_{EM}}\left[n'_{k+k_p} + n'_{k-k_p}\right] \tag{10}$$

where $\epsilon_{EM} = ((k^2c^2/\omega^2) + (\omega_{pe}^2/\gamma_0\omega^2) - 1)$ is defined as the electromagnetic dielectric function. From $\boldsymbol{E} = -\nabla\Phi - (1/c)(\partial\boldsymbol{A}/\partial t)$, we write

$$E'_{x,k} = \frac{i\omega}{c}A'_{x,k}. \tag{11}$$

From the linearized equation of continuity

$$\frac{\partial n'}{\partial t} + v_{0z}\frac{\partial n'}{\partial z} + n_0\frac{\partial v'_z}{\partial z} = 0 \tag{12}$$

and Poisson's equation

$$\frac{\partial E'_z}{\partial z} = -4\pi e n' \tag{13}$$

we can derive

$$n'_{k+k_p} = \frac{k + k_p}{\omega - v_{0z}(k + k_p)}v'_{z,k+k_p} \tag{14}$$

$$n'_{k+k_p} = \frac{i(k + k_p)}{4\pi e}E'_{z,k+k_p} \tag{15}$$

and

$$E'_{z,k+k_p} = \frac{i4\pi e n_0}{\omega - v_{0z}(k + k_p)}v'_{z,k+k_p} \tag{16}$$

where $k_p = \omega_p/c$. Equations (8), (12), and (13), together with (23), which is derived later on, form a closed set of equations that can be used to determine the dispersion relation.

Once there is spontaneous emission at ω ($\sim 2\gamma_0^2\omega_p$), there is resonant ponderomotive force on the radiating electrons. This force is $\boldsymbol{F} = -(e/c)\boldsymbol{v}_\omega \times \boldsymbol{B}_r$, where $\boldsymbol{v}_\omega$ is the quiver velocity and $\boldsymbol{B}_r$ is the magnetic field of the spontaneous or stimulated radiation. For a radiation field

$$\boldsymbol{B}_r = \frac{ck}{\omega} E_r \cos(kz - \omega t + \phi)\boldsymbol{a}_y \tag{17}$$

together with (1), the ponderomotive force is

$$F_z = -\frac{1}{2}\left(\frac{eE_p}{m_0\gamma_0\omega_p}\right)\left(\frac{ekE_r}{\omega}\right) \cdot \left\{\cos\left[kz - (\omega - \omega_p)t + \phi\right] + \cos\left[kz - (\omega + \omega_p)t + \phi\right]\right\} \tag{18}$$

where ϕ is the phase difference between the electron and the electromagnetic field. The second term in (18) has a phase velocity slightly greater than c and thus its time-averaged value is zero; therefore we discard this term [16]. When the electrons must have velocities in a range that is slightly greater than the phase velocity of the ponderomotive bucket, a net energy exchange from the electron beam to the radiation would be obtained. Using $\boldsymbol{B} = \nabla \times \boldsymbol{A}$ and $\boldsymbol{E} = -\nabla\Phi - (1/c)(\partial \boldsymbol{A}/\partial t)$, we obtain

$$E_x = E_r \cos\left[kz - \omega t + \phi\right]. \tag{19}$$

Equations (10), (11), and (15) yield

$$E'_{x,k} = -\frac{eE_p(k + k_p)}{2m_0\gamma_0\omega_p\omega\epsilon_{\text{EM}}} E'_{z,k+k_p} \tag{20}$$

which relates the amplitude of the electromagnetic wave to the amplitude of the electrostatic wave.

From (19) and (20), we can write

$$E'_z = E'_0 \cos\left[(k + k_p)z - \omega t + \phi\right] \tag{21}$$

where

$$E'_0 = -\frac{2m_0\gamma_0\omega_p\omega E_r\epsilon_{\text{EM}}}{eE_p(k + k_p)}. \tag{22}$$

The longitudinal component of the linearized equation of motion is

$$m_0\gamma_0^3\left(\frac{\partial}{\partial t} + v_{0z}\frac{\partial}{\partial z}\right)v'_z = -eE'_z + F_z - \frac{3k_BT}{n_0}\frac{\partial n'}{\partial z} \tag{23}$$

where T is the absolute temperature and k_B is Boltzmann's constant. The solution of (23) is

$$v'_z = \frac{e\tilde{E}_0}{m_0\gamma_0^3 Q}\sin\left[(k + k_p)z - \omega t + \phi\right] \tag{24}$$

where

$$\tilde{E}_0 = E'_0 + \frac{1}{2}\left(\frac{eE_p}{m_0\gamma_0\omega_p}\right)\left(\frac{kE_r}{\omega}\right)$$

$$Q = \omega - (k + k_p)\left\{v_{0z} + \frac{3(k + k_p)k_BT}{m_0\gamma_0^3\left[\omega - v_{0z}(k + k_p)\right]}\right\}.$$

Substituting (21) and (24) into (16) finally yields the dispersion relations, given by

$$D_{\text{ES}}(k, \omega)D_{\text{EM}}(k, \omega) = F \tag{25}$$

where

$$D_{\text{ES}}(k, \omega) = \left[\omega - v_{0z}(k + k_p)\right]^2 - \frac{\omega_{pe}^2}{\gamma_0^3}\left[1 + 3(k + k_p)^2\lambda_D^2\right]$$

$$D_{\text{EM}}(k, \omega) = \left[\omega^2 - k^2c^2 - \frac{\omega_{pe}^2}{\gamma_0}\right]$$

$$F = \frac{e^2E_p^2\omega_{pe}^2 k(k + k_p)}{4m_0^2\gamma_0^5\omega_p^2}$$

and λ_D is the Debye length.

The dispersion relation shows that the plasma oscillations are coupled to the electromagnetic waves through the spatially uniform and transversely oscillating electric field. For the uncoupled electrostatic and electromagnetic waves, the electromagnetic mode is

$$\omega^2 - k^2c^2 = \frac{\omega_{pe}^2}{\gamma_0} \tag{26}$$

and the positive- and negative-beam space-charge modes are ($k_p = 0$)

$$\omega = kv_{0z} \pm \frac{\omega_{pe}}{\gamma_0^{3/2}}\left[1 + 3k^2\lambda_D^2\right]^{1/2}. \tag{27}$$

There is no interaction and no instability in the uncoupled state of the system. Instability will occur if the negative-energy space-charge mode interacts with the positive-energy electromagnetic mode. The wiggler electric field modifies (27) as

$$\omega = (k + k_p)v_{0z} \pm \frac{\omega_{pe}}{\gamma_0^{3/2}}\left[1 + 3(k + k_p)^2\lambda_D^2\right]^{1/2} \tag{28}$$

so that there now exists the possibility of coupling and instability.

The dispersion relation is a fourth-order equation in ω. If the coupling term is much less than unity, then the dispersion relation may be expanded around the natural frequencies according to

$$\omega = \omega_1 + \delta = \omega_2 + \delta + \mu \tag{29}$$

where

$$\omega_1 = \left(k^2c^2 + \frac{\omega_{pe}^2}{\gamma_0}\right)^{1/2}$$

$$\omega_2 = (k + k_p)v_{0z} - \frac{\omega_{pe}}{\gamma_0^{3/2}}\left[1 + 3(k + k_p)^2\lambda_D^2\right]^{1/2}$$

and μ is the frequency mismatch between the electrostatic and electromagnetic waves in the absence of the wiggler electric field. Substituting (29) into (25), after some manipulation, yields

$$\omega = \omega_1 + \frac{1}{2}\left\{ -\mu \pm i \cdot \left[\frac{e^2\omega_{pe}^2 E_p^2 k(k + k_p)}{4m_0^2\gamma_0^{7/2}\omega_p^2\omega_1[1 + 3(k + k_p)^2\lambda_D^2]} - \mu^2 \right]^{1/2} \right\}. \quad (30)$$

This equation indicates that the electromagnetic wave is unstable and the width of the unstable spectrum is determined by such parameters as γ_0, E_p, and ω_p.

The growth rate is finally given by

$$\omega_i = \frac{1}{2}\left\{ \frac{e^2\omega_{pe}E_p^2 k(k + k_p)}{4m_0^2\gamma_0^{7/2}\omega_p^2\omega_1[1 + 3(k + k_p)^2\lambda_D^2]} - \mu^2 \right\}^{1/2}. \quad (31)$$

The growth rate is linearly dependent on the strength of the electric field.

Next, we derive the ratio of the electromagnetic to the electrostatic wave energy. In order to have high efficiency in energy conversion from the beam to the electromagnetic radiation, it is necessary that the electron beam lose a large fraction of its energy during the instability. From (10), (11), and (15), the amplitude of the electromagnetic wave can be written in terms of the amplitude of the electrostatic wave:

$$E'_{x,k} = -\frac{eE_p(k + k_p)}{2m_0\gamma_0\omega_p\omega\epsilon_{EM}} E'_{z,k+k_p}. \quad (32)$$

Since the unstable electromagnetic waves satisfy the electromagnetic dispersion relation approximately, we can write

$$\epsilon_{EM}(k, \omega) = \epsilon_{EM}(k, \omega_R) + i\omega_i \left.\frac{\partial\epsilon_{EM}(k, \omega)}{\partial\omega}\right|_{k,\omega_R} \quad (33)$$

where $\epsilon_{EM}(k, \omega_R) = 0$ and $\omega = \omega_R + i\omega_i$. Thus

$$\epsilon_{EM}(k, \omega) = i\omega_i \left.\frac{\partial\epsilon_{EM}(k, \omega)}{\partial\omega}\right|_{k,\omega_R} = -\frac{2i\omega_i}{\omega_R}. \quad (34)$$

From (32) and (34), the energy of the unstable electromagnetic wave is

$$W_{EM} = \frac{1}{2}\left[\frac{eE_p(k + k_p)}{2m_0\gamma_0\omega_p\omega_i}\right]^2 W_{ES}$$

where $W_{EM} = (1/4\pi)E'^2_{x,k}$ and $W_{ES} = (1/8\pi)E'^2_{z,k+k_p}$ are the energies of the electromagnetic and electrostatic waves. The ratio of the electromagnetic to the electrostatic wave energy is

$$\frac{W_{EM}}{W_{ES}} = \frac{1}{2}\left[\frac{eE_p(k + k_p)}{2m_0\gamma_0\omega_p\omega_i}\right]^2 \quad (35)$$

which is much larger than unity for all the cases we consider.

In the cold beam, weak pump, Raman regime, the dominant saturation mechanism appears to be electron trapping in the electrostatic idler wave. As the interaction proceeds and the beam loses energy, the space-charge wave will eventually reach an amplitude at which it can trap most of the electrons. Hence, at the trapping time the electron beam velocity, on the average, is approximately equal to the phase velocity of the space-charge wave.

Since the group velocity of the scattered electromagnetic wave and the velocity of the electron beam in the laboratory frame are very nearly equal to the velocity of light, the efficiency of stimulated backscattering is defined as the ratio of the average electromagnetic energy density in the laboratory frame to the kinetic energy density of the electrons [3]. Assuming that all the energy lost from the electron beam is converted into electromagnetic radiation, the efficiency, $\bar{\eta}$, is approximately given by

$$\bar{\eta} \approx \frac{|\Delta W|}{m_0c^2(\gamma_0 - 1)} = \frac{\gamma_0 - \gamma_{ph}}{\gamma_0 - 1} \quad (36)$$

where $\Delta W = m_0c^2(\gamma_0 - \gamma_{ph})$ is the change in the energy of the electron beam, and $\gamma_{ph} = [1 - (v_{ph}/c)^2]^{-1/2}$ is the relativistic factor corresponding to the phase velocity of the ponderomotive wave.

From (28), the phase velocity of negative-energy space charge mode is

$$v_{ph} = \frac{\omega}{k + k_p} = v_{0z} - \frac{\omega_{pe}}{\gamma_0^{3/2}(k + k_p)}. \quad (37)$$

Assuming γ_0 is large and using $k \sim 2\gamma_0^2 k_p$ yields the efficiency, given by

$$\bar{\eta} \approx \frac{\omega_{pe}}{2\gamma_0^{3/2}k_p c}. \quad (38)$$

Fig. 4 and Figs. 7–9 illustrate its dependence on the relativistic factor γ_0.

III. Gain Calculation

The Lorentz equation is written as

$$mc^2 \frac{d\gamma}{dt} = -e\vec{E} \cdot \vec{v} \quad (39)$$

where $\vec{E}$ is the electric field of the electromagnetic wave of (19).

The first-order perturbation equation of γ caused by the electromagnetic wave is

$$mc^2 \frac{d\gamma_1}{dt} = -e\vec{E}_r \cdot \vec{v}_\omega = -ev_x E_r \cos(kz - \omega t + \phi). \quad (40)$$

Integrating (40) in the interaction region $[0, L]$, we have

$$\gamma_1 = -\frac{ev_\omega E_r}{2mc^2 v_{0Z}} \frac{\sin(\Delta kL + \phi) - \sin\phi}{\Delta k}$$

where

$$\Delta k = k - \frac{\omega - \omega_p}{v_{0Z}}.$$

Squaring γ_1 and averaging over ϕ gives

$$\langle \gamma_1^2 \rangle = \frac{L^2}{2} \left(\frac{eE_r v_\omega}{2mc^2 v_{0z}} \right)^2 \frac{\sin^2}{U^2} U \tag{41}$$

where

$$U = \frac{L}{2} \Delta k.$$

According to the Madey theorem [4], we obtain a second-order perturbation of γ:

$$\langle \gamma_2 \rangle = \frac{1}{2} \frac{d}{d\gamma} \langle \gamma_1^2 \rangle. \tag{42}$$

The gain is written as [5]

$$G = \frac{-\langle \gamma_2 \rangle mc^2 I/e}{\frac{1}{2}\epsilon_0 E_r^2 c A_\omega} \tag{43}$$

where A_ω is the area of the optical wave and I is the electron beam current. The final form for the gain is

$$G = \frac{1}{8} \left(\frac{\mu_0}{\epsilon_0} \right)^{1/2} \frac{Ie}{mc^2} \left(\frac{a_\omega}{\gamma_0} \right)^2 \frac{L^2 k L (1 + a_\omega^2)}{A_\omega \beta_z^5 \gamma_0^3} \frac{d}{dU} \left(\frac{\sin^2 U}{U^2} \right). \tag{44}$$

We can also define the rate of amplification of radiative energy per unit length of the interaction domain. This rate of amplification per unit length can be written in terms of commonly used parameters for the expression of the FEL gain [6] as

$$g = \frac{3}{64\pi^2 \epsilon_0} n_b \sigma_T \frac{E_p^2}{mc^2} \tau \frac{\lambda_p L^2}{\gamma_0^3} (1 + a_\omega^2) \frac{d}{dU} \left(\frac{\sin^2 U}{U^2} \right) \tag{45}$$

where $\lambda_p = 2\pi/k_p$, σ_T is the Thomson cross section, and τ is the ratio of the effective cross section of the electron beam to that of the electromagnetic wave.

It should be noted that the gain formulas given by (44) and (45) are valid only for the small-signal gain regime.

IV. Results

A. ac FEL

We use an Astron beam [15] as an example of a feasible electron beam to determine what we might expect from the ac FEL. Typical Astron-beam parameters have the following values: density $n_b = 3 \times 10^{12}$ cm^{-3}, relativistic factor $\gamma_0 = 10$, energy spead $\Delta\gamma_0/\gamma_0 \approx 10^{-3}$, and Debye length $\lambda_D \sim 1$ μm. We adopt an ac electric field of frequency $f_0 = 5$ GHz with amplitude $E_p = 20$ MV/m ($\epsilon_0 = eE_p/m_0 c\omega_{pe} = 0.12$).

First, we investigate the dependence of the growth rate on the relativistic factor, γ_0. In Fig. 2, the growth rates are plotted against wavenumbers for $\gamma_0 = 9$, 10, and 11. The growth rate decreases monotonically as a function of γ_0. Second, we illustrate the dependence of the growth rate on the strength of the electric field ranging from $\epsilon_0 =$ 0.04 to 0.12 in Fig. 3. The growth rate and the width of the unstable spectrum are linearly dependent on the amplitude of the electric field. Third, the dependence of the efficiency on the relativistic factor γ_0 is shown in Fig. 4. As previously seen in (38), the efficiency decreases monotonically as a function of γ_0.

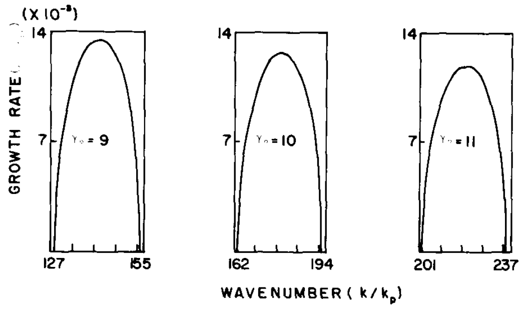

Fig. 2. Theoretical growth rate as a function of wavenumber for different beam energies.

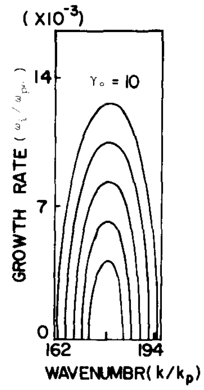

Fig. 3. Theoretical growth rates ranging from $\epsilon_0 = 0.04$ to 0.12 are shown as a function of wavenumber.

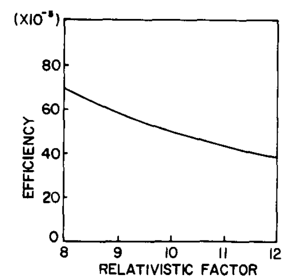

Fig. 4. Efficiency of radiation production as a function of the relativistic factor γ_0.

B. FEL with Plasma Wave Wiggler

In this case, the parameters have the following values [16]: wiggler strength a_ω ($= eE_p/m_0 c\omega_p$) $= 0.1$, plasma density $n_0 = 10^{17}$ cm^{-3}, beam densities $n_b = 1.5 \times 10^{15}$ cm^{-3}, 3.6×10^{15}, and 5.4×10^{16} for relativistic factor $\gamma_0 = 15$, 20, and 50, respectively.

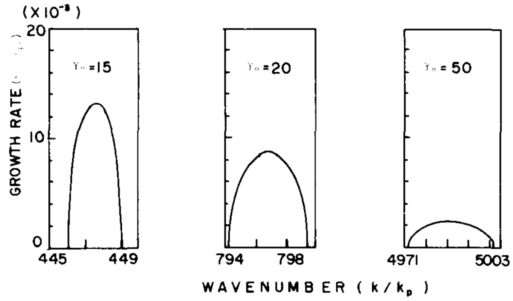

Fig. 5. Theoretical growth rate as a function of wavenumber for different beam energies.

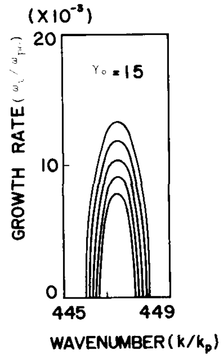

Fig. 6. Theoretical growth rates for the wiggler strength from $a_\omega = 0.06$ to 0.1 are shown as a function of wavenumber.

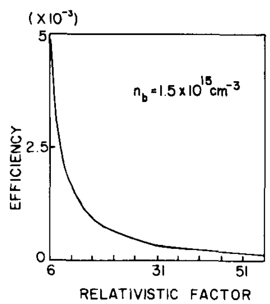

Fig. 7. Efficiency of radiation production as a function of relativistic factor γ_0.

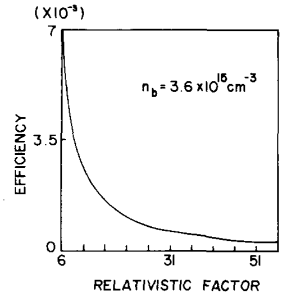

Fig. 8. Efficiency of radiation production as a function of relativistic factor γ_0.

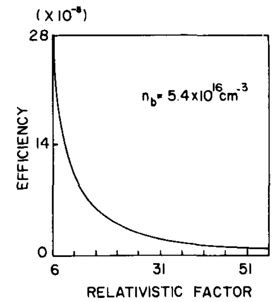

Fig. 9. Efficiency of radiation production as a function of relativistic factor γ_0.

In Fig. 5, the growth rates are plotted against wavenumbers for $\gamma_0 = 15$, 20, and 50. The growth rate also decreases monotonically as a function of γ_0. Fig. 6 shows the dependence of the growth rate on the wiggler strength, a_ω, ranging from 0.06 to 0.1. The growth rate and the width of the unstable spectrum are also linearly dependent on the wiggler strength, a_ω. Figs. 7, 8, and 9 show the dependence of the efficiency on the relativistic factor γ_0 for $n_b = 1.5 \times 10^{15}$ cm^{-3}, 3.6×10^{15}, and 5.4×10^{16}, respectively. The efficiency is enhanced by the beam density.

It should be noted that in this case the whole wiggler plasma is assumed to be oscillating coherently and the electron beam–plasma interaction is suppressed considerably.

V. Conclusions

In this study, an ac FEL with the superconductor cavity and a FEL with plasma wave wiggler are analyzed. The ac FEL has drawn interest because of its small effective wiggler wavelength and high wiggler strength. Therefore it can supply high-power coherent radiation with a short wavelength.

From the linear fluid theory and Maxwell's equations, we derive the dispersion relation. When the coupling term is much less than unity ($F << 1$), we calculate the growth rate of the electromagnetic instability. The intrinsic efficiency of radiation production is also estimated. Finally, for the small-signal gain regime, we formulate the gain coefficient based on the Madey theorem.

In a FEL with plasma wiggler, the electron beam passing through the wiggler plasma might begin to thermalize due to various particle–particle and wave–particle interactions. Thus the effective interaction region becomes contracted, which prevents the coherence of the electromagnetic wave. To avoid such interactions, the electron beam should be bunched and narrower than the skin depth.

The parameters employed for the numerical illustration of various characteristics of the FEL pertain to an ongoing experiment. From the results we can note the followings: The growth rate has a linear dependence on the amplitude of the electric wiggler and decreases with increasing beam energy. The intrinsic efficiency of radiation production decreases with increasing beam energy. In a FEL with the plasma wiggler, the efficiency is shown to be enhanced by an increase in the electron beam density.

ACKNOWLEDGMENT

The authors wish to thank Prof. G. S. Cho of Inje University for valuable discussions.

REFERENCES

[1] P. C. Efthimion and S. P. Schlesinger, *Phys. Rev. A*, vol. 16, p. 633, 1977.
[2] N. M. Kroll and W. A. McMullin, *Phys. Rev. A*, vol. 17, p. 300, 1978.
[3] P. Sprangle and A. T. Drobot, *J. Appl. Phys.*, vol. 50, p. 2652, 1979.
[4] J. M. J. Madey, *Nuovo Cimento*, vol. 50B, p. 64, 1979.
[5] L. K. Grover and R. H. Pantell, *IEEE J. Quantum Electron.*, vol. QE-21, p. 944, 1985.
[6] S. Ichimaru and N. Iwamoto, *J. Phys. Soc. Japan.*, vol. 44, p. 1004, 1978.
[7] T. Kwan, J. M. Dawson, and A. T. Lin, *Phys. Fluids*, vol. 20, p. 581, 1977.
[8] P. Sprangle and R. A. Smith, *Phys. Rev. A*, vol. 21, p. 293, 1980.
[9] R. B. Miller, *An Introduction to the Physics of Intense Charged Particle Beams.* New York: Plenum, 1982, pp. 248–265.
[10] T. Kwan and J. M. Dawson, *Phys. Fluids*, vol. 22, p. 1089, 1979.
[11] L. Friedland and A. Fruchtman, *Phys. Rev. A*, vol. 25, p. 2693, 1982.
[12] L. Friedland and I. B. Bernstein, *Phys. Rev. A*, vol. 26, p. 2778, 1982.
[13] H. P. Freund, R. A. Kehs, and V. L. Granatstein, *Phys. Rev. A*, p. 2007, 1986.
[14] T. P. Pandya, L. M. Bali, U. Bakshi, and P. Jha, *Phys. Rev. A*, vol. 35, p. 5131, 1987.
[15] Y. T. Yan and J. M. Dawson, *Phys. Rev. Lett.*, vol. 57, p. 1599, 1986.
[16] C. Joshi, T. Katsouleas, J. M. Dawson, Y. T. Yan, and J. M. Slater, *IEEE J. Quantum Electron.*, vol. QE-23, p. 1571, 1987.

Tae Hun Chung was born in Pusan, Korea, on February 14, 1958. He received the B.E. (nuclear engineering, 1982) degree from Seoul National University and the M.S.E. (nuclear engineering, 1984) and Ph.D. (nuclear engineering, 1986) degrees from the University of Michigan, Ann Arbor. While at the University of Michigan, he studied plasma physics, fusion engineering, and the quantum theory of radiation. His doctoral research was on the quantum theory of the microwave heating of plasma.

In September 1986 he became an Assistant Professor at Dong-A University, Pusan, Korea. His research interests presently center on free electron lasers and the theoretical study of high-power radiation sources.

*

Jin Hyun Lee was born in Pusan, Korea, on July 10, 1963. He received the B.S. degree in physics from Dong-A University, Pusan, Korea, in 1986 and the M.S. degree there in 1989. His graduate studies included plasma physics and the theory of high-power radiation sources. He is currently involved in computer simulation studies of the free electron laser.